13th World Conference on Earthquake Engineering
Vancouver, B.C., Canada
August 1-6, 2004
Paper No. 1721

DISTRIBUTION OF PEAK HORIZONTAL FLOOR ACCELERATION FOR ESTIMATING NONSTRUCTURAL ELEMENT VULNERABILITY

Samit RAY CHAUDHURI[1] and Tara C. HUTCHINSON[2]

SUMMARY

Peak horizontal floor acceleration (PHFA) is now widely used by the engineering community for estimating the vulnerability of both attached and unattached acceleration sensitive nonstructural elements. Recent performance-based earthquake engineering approaches have cast this estimation in a probabilistic form, where seismic fragility curves are used to represent the probability that a specific damage measure (DM) will occur, given an earthquake of a specified intensity. Since both attached and unattached nonstructural elements are generally placed at various levels of a building structure, PHFA is taken as the engineering demand parameter (EDP) and placed as the abscissa in these curves. To estimate the force imposed on attached nonstructural elements such as architectural, mechanical and electrical components, PHFA is assumed to vary with the height of the building. Since the peak horizontal floor acceleration at a particular level of the building depends on the dynamic characteristics of the building, the level of nonlinearity induced, and the ground excitation, PHFA cannot be generalized as a function of height without considering these aspects. In this study, the distribution of absolute acceleration amplification Ω (PHFA normalized by peak ground acceleration) along the height of buildings with different dynamic characteristics is developed through nonlinear regression analysis. Numerical models of a total of eight moment-resisting steel frame buildings (flexible and rigid), representing actual buildings on the West Coast of the U.S., are constructed. An ensemble of thirty-two different ground motions, representing hazard levels of 2, 10, and 50% probability of exceedance are used as input to the building models and nonlinear dynamic analysis conducted. Resulting distributions are compared with code-recommendations and a simplified distribution of Ω is proposed, based on assumed physical contributions to the behavior and regression through the dynamic analyses results. Although simplified, the suggested distribution of Ω will lead to more reliable estimates of the vulnerability of acceleration sensitive nonstructural components.

INTRODUCTION

It is now widely recognized that the effect of failure of nonstructural components is significant during any earthquake. As a result, economic loss due to nonstructural component damage has been considerable. Losses due to nonstructural components have consistently been reported to be far greater than those resulting from structural damage (Ayers [2,3], Whitman [25], Rihal [13]). Investigations have also reported that damage to nonstructural components and building contents during recent earthquakes in the U.S. have resulted in unprecedented economic losses (Soong [20, 21], Reitherman [12], Phipps [11]). The importance of failure of nonstructural components was widely recognized after the 1971 San Fernando earthquake, after which it was recognized that the damage of nonstructural components may not only

---

[1] Doctoral Candidate, Department of Civil and Env. Engineering, Univ. of California, Irvine, USA. 92697-2175
[2] Assistant Professor, Department of Civil and Env. Engineering, Univ. of California, Irvine, USA. 92697-2175

result in major economic loss but also poses a threat to life. In addition, the potential loss of functionality of buildings due to damage to nonstructural components has recently received special attention. Due to the numerous types of nonstructural systems within critical facilities such as hospitals, fire and police stations, power generation facilities, water supply and water treatment facilities, their vulnerability for functionality loss is significantly higher. Moreover, fire hazards resulting from sliding, toppling and breaking of chemical storage containers or glassware resting on furnishings are very high. During the 1994 Northridge earthquake several major hospitals had to be evacuated not due to structural damage but because of the damage caused by failure of water lines and water supply tanks; the failure of emergency power systems and heating, ventilation, and air conditioning units; damage to suspended ceilings, and light fixtures; and some broken windows.

The numerous types of nonstructural components found within any typical building structure makes the evaluation of their response and impact on the structure a difficult task. A common approach is to classify these components and systems as either acceleration-sensitive or deformation-sensitive, based on the input, which governs their response. Components such as; suspended ceilings, bookshelves, file cabinets, storage racks, emergency power generation systems, light fixtures, rigid attached nonstructural components such as air conditioning units, cable trays and control panels, bench mounted scientific equipment such as analyzer, microscopes, chemical glassware, and others, are generally classified as acceleration sensitive nonstructural components and thus damaged primarily as a result of being subjected to large floor accelerations. As a result of the large number of nonstructural components, which may be classified as acceleration sensitive, the determination of accurate floor level acceleration in a building when subjected to an earthquake is very important for estimating the vulnerability and reducing the risk of failure of nonstructural components.

Although the significance of the survival of nonstructural components is well understood, limited research has been conducted to understand and mitigate their vulnerability. Present seismic design provisions (e.g. UBC [24], NEHRP [9]) recommend a linear variation of acceleration along the height of the building to estimate the design force induced on the nonstructural components. The design philosophy adopted by the UBC and NEHRP provisions seeks to assure that these components will be designed such that they will be able to withstand the design earthquake load without collapse, toppling or shifting. Such a philosophy is common to the design of building structures. Using the guidelines, an equivalent lateral load is determined as a function of an element's weight, anticipated ground acceleration, location of the element within the building, the element's dynamic amplification, and the element's ability to absorb inelastic deformations. The inelastic behavior of the support structure has not been included in codified formulas because it is to be believed that: (i) the extent of inelastic behavior is usually minor for structures designed by modern building codes, as their design is in many case governed by drift limits or other loads; (ii) nonstructural components are often designed without knowledge of the structure's composition; and (iii) it is a conservative consideration. Comparing the UBC 1997 code recommendations, one notes that the calculation of forces applied to nonstructural components assumes a trapezoidal distribution of acceleration, varying with the PGA (Peak ground acceleration) at the ground level to four times the PGA at the roof level. In contrast, the NEHRP 2000 assumes a linear variation, with the PGA at the ground level to three times the PGA at the roof level. The provisions used in UBC and NEHRP were developed empirically on the basis of floor acceleration data recorded in buildings during California earthquakes (Kehoe [6]). Codified formulas also recommend the same distribution along the height of a building, regardless of the number of stories in the building, its lateral resisting system or expected nonlinear behavior. As a consequence, it is not known whether or not a nonstructural component designed with these formulas will be able to resist a large earthquake (Soong [21]). Kehoe [6] and Searer [16] concluded that the intensity and distribution of floor accelerations over the height of a building is influenced by the predominant period of vibration of the building, the mode shapes and their relative contributions. However, their conclusions are based on earthquakes, which were not strong enough to induce nonlinear deformations. Miranda [8] presented a simplified method for estimating floor acceleration distribution of elastic buildings when subjected to a particular ground motion. However, this work also did not consider nonlinear behavior of the building, which is very common when subjected to large earthquakes. Several investigations have pointed out that the nonlinear behavior of a building and nonstructural system may significantly affect the response of nonstructural systems, either by significantly reducing or substantially amplifying the response, as compared with the corresponding linear response (e.g. Lin [7], Aziz [4], Toro [22], Sewell [17], Igusa [5], Singh [18], Schroeder [15], and Adam [1]).

Scope of this Paper

In this study, the distribution of the peak horizontal floor acceleration (PHFA) along the height of building structures is investigated assuming a large number of ground motions, with a broad range of seismic hazard levels. For this purpose, eight representative steel moment-resisting frame buildings are considered and numerical models constructed using OpenSees [10]. An ensemble of 32 different earthquake time histories is used as input to the numerical models with nonlinearity incorporated at beam-column joints, as commonly anticipated in design practice. Although there is significant scatter in the resulting acceleration amplification distribution, a lognormal distribution on a per floor basis is shown to reasonably estimate the ensemble floor distributions. Using the lognormal assumption, confidence levels are calculated compared with the UBC and NEHRP code recommendations. Finally, a proposed acceleration distribution, with an associated confidence level, is presented such that the probability of exceeding a limit state of Ω is reduced considering all floors. The proposed acceleration amplification distribution will lead to more reasonable estimations of the vulnerability of acceleration sensitive nonstructural components.

REPRESENTATIVE BUILDINGS AND THEIR NUMERICAL MODELS

For this study, eight steel moment-resisting frame (SMRF) buildings with four, eight, twelve and sixteen stories are considered. The eight buildings, previously considered by Santa-Ana [14], have the same square floor plan of 21.94m x 21.94m consisting of three bays in each horizontal direction at an interval of 7.3 m. The buildings have a uniform mass distribution over their height and a non-uniform lateral stiffness distribution. They were designed using the lateral load distribution specified in the 1994 UBC [23] with member stiffness tuned to obtain fundamental periods of vibration for each structure representative of those obtained from earthquake records of instrumented existing SMRFs. Figure 1(a)-(h) shows the representative exterior frames of each of these buildings. Excluding the beam-to-column connections in the top floor, the steel sections of the structural members were selected such that the sum of the plastic moments of the columns framing into each beam-column joint was higher than the sum of plastic moments of the beams framing into the same joint.

Numerical models were developed in OpenSees [10] for these structures, using a representative 2D frame of the buildings along the transverse direction (as shown in Figure 1). Apart from geometric nonlinearity, the two buildings material nonlinearity comes from the beams, at their connection with the columns. The buildings are assumed as fixed base and a lumped mass model is developed. Two percent Rayleigh damping is considered and 3% kinematic material hardening is considered for the nonlinear beams and columns.

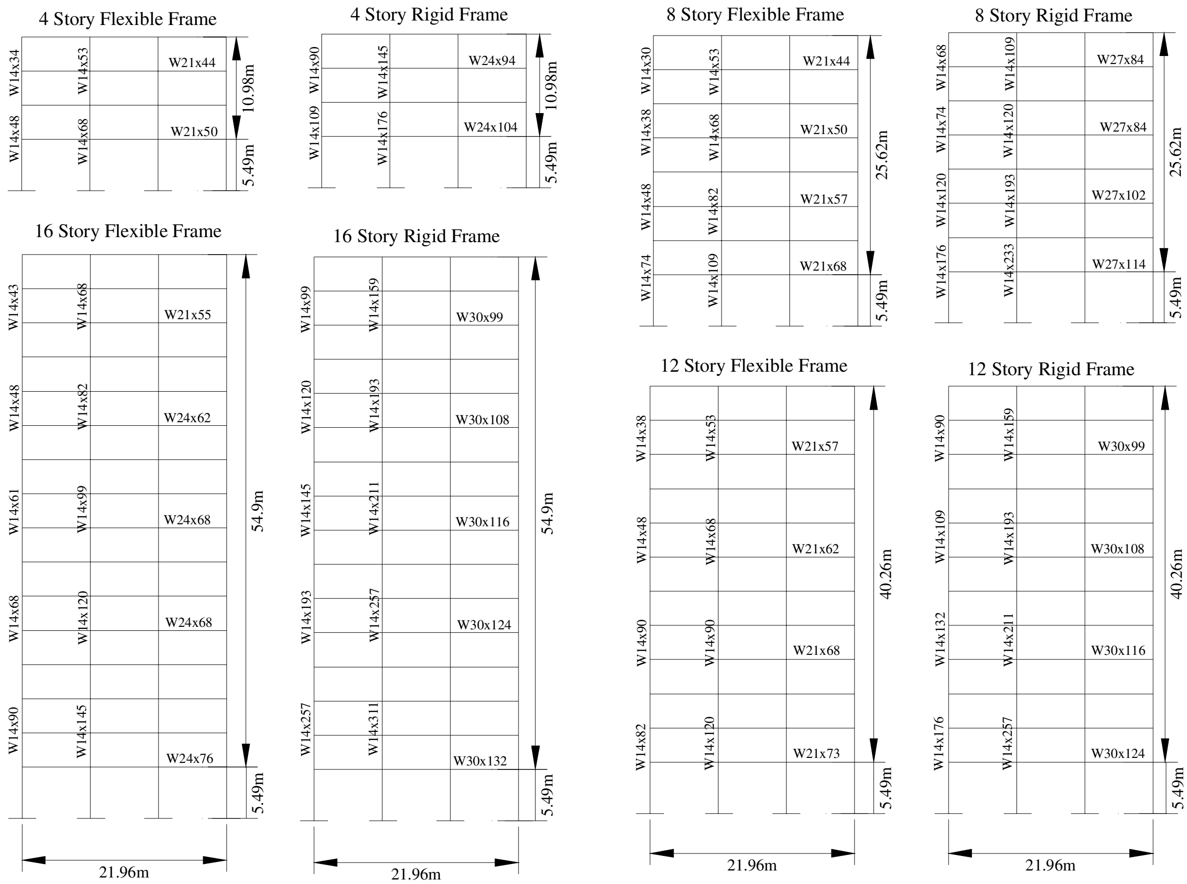

Figure 1. Representative exterior frames of all eight buildings considered in this study.

RESULTS AND DISCUSSION

Eigenvalue and Nonlinear Pushover Analysis

Results from an eigenvalue analysis of the different models, including the first (fundamental), second and third mode periods of vibration for all structures are provided in Table 1. The calculated fundamental periods of these structures is broad, ranging from T_1= 0.71 – 3.09 seconds. In addition, the first effective modal mass (M^*) normalized by the total mass of the systems (M_T) is noted. It may be observed that the normalized modal masses decrease with the number of stories and are slightly larger for the flexible frames than for the rigid frames.

Static nonlinear pushover analysis is performed to obtain the roof displacement versus base shear capacity for the building frames. To carry out the pushover analysis, load is applied following the first mode shape pattern. To solve the nonlinear equations, the Newton-Rapson iteration algorithm is used. Figure 2(a) shows an example of the pushover curves for the 4 story building frames considered in this study (flexible and rigid). The yield point in this case is defined as the point on the pushover curve where separation from the elastic response is observed. It is interesting to note that both models yield at nearly same drift level. Table 1 summarizes the roof level yield displacement Δ_y, the ratio of Δ_y to the total height of building (the yield drift ratio) Γ_y, the base shear at yield V_y, and associated acceleration at yield A_y (which is obtained by dividing the base shear at yield by the total mass of the frame (= V_y / M_T)). It is interesting to note that the yield drift ratio is close to 1% for all buildings. This signifies that these building are designed with a drift limit of approximately 1% to remain elastic. Figure 2(b) summarizes the calculated capacity estimates (in terms of A_y and Δ_y) for each building as a function of fundamental period. It may be observed from this figure that as the period increases, the yield acceleration, A_y decreases, while the yield displacement Δ_y increases, for both the rigid and flexible frames.

Table 1. Characteristics of the building frames considered in this study.

Type of Building	Dynamic characteristics				Capacity Characteristics			
	First natural period (s)	Second natural period (s)	Third natural period (s)	M^*/M_T	Δ_y (cm)	Γ_y (%)	V_y (kN)	A_y (g)
4 story flexible	1.23	0.39	0.20	0.98	15.27	0.93	75.85	0.30
4 story rigid	0.71	0.22	0.12	0.97	16.38	0.90	261.10	1.03
8 story flexible	1.92	0.68	0.39	0.95	35.31	1.14	128.90	0.25
8 story rigid	1.18	0.42	0.24	0.92	35.10	1.13	336.10	0.66
12 story flexible	2.61	0.91	0.53	0.89	37.59	0.82	109.40	0.14
12 story rigid	1.53	0.53	0.31	0.88	41.48	0.91	349.50	0.46
16 story flexible	3.09	1.00	0.55	0.87	76.50	1.27	195.60	0.19
16 story rigid	1.87	0.61	0.34	0.86	64.62	1.07	457.00	0.45

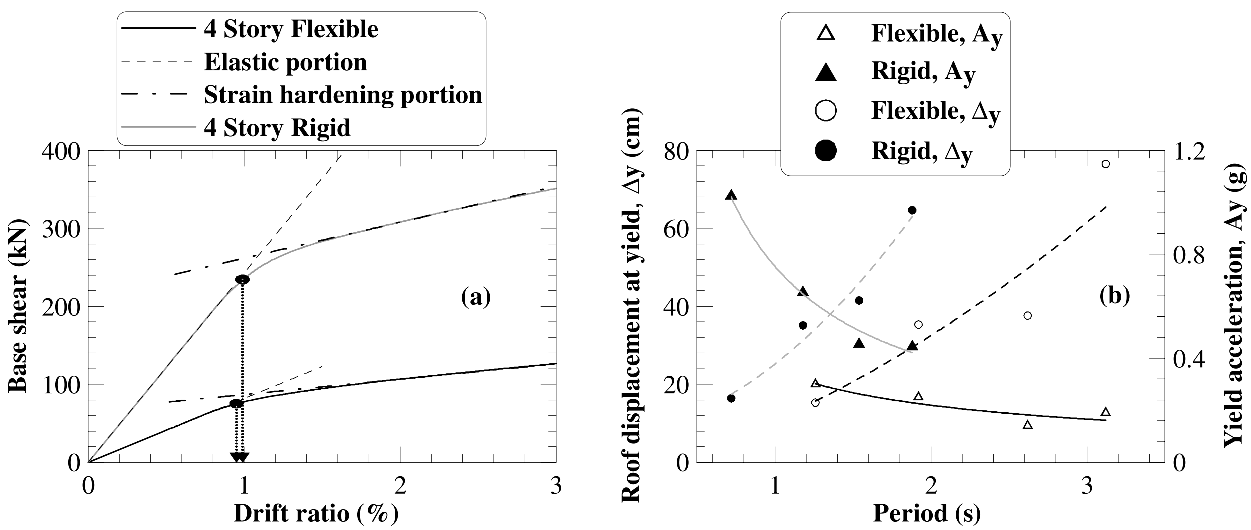

Figure 2. Nonlinear pushover results: (a) example of parameter estimation for 4 story flexible and rigid frames and (b) summary of calculated capacities (in terms of A_y and Δ_y).

Ground Motions Considered

A suite of ground motions, corresponding to a scenario earthquake, is a common approach for estimating the fragility of both structural and nonstructural systems at a given site. Such an ensemble is often generated by scaling appropriate recordings to match site-specific response spectral ordinates, corresponding to assumed period. In a similar fashion, for this study, 22 measured ground motions are scaled to different hazard levels of 50, 10, and 2% in 50 years, resulting in a total of 32 input motions (Sommerville 2002). These ground motion were generated for the UC Science building as a part of PEER (Pacific Earthquake Engineering Research Center) test bed project. Hazard level scale factors were determined by matching site-specific spectral ordinate at a period of 0.45 seconds. The ground motions are derived from actual ground motion records considering their magnitude and distance from the fault to site at which records are collected. The list of the ground motions used along with their different peak parameters is provided in Table 2. The peak ground acceleration (PGA) for these motions varies from 0.26g to 2.5g. The range of peak ground velocity (PGV) is PGV = 14 – 260.5 cm/sec, and the range of peak ground displacements (PGD) is PGD = 1.2 – 141.2 cm. In addition to the broad hazard levels, these motions represent a variety of characteristics, including different peak parameters and dominant frequency content.

The variation of these ground motions may be observed by binning their acceleration and displacement response spectrum into respective hazard levels. Assuming 2% damping, Figure 3(a)-(c) shows the mean m and mean plus one standard deviation (m+σ), acceleration spectra, while (d)-(f) shows the m and (m+σ) displacement spectra for 2%, 10%, and 50% in 50 year hazard levels, respectively. From these plots, it is clear that significant variation is inherent among this ground motion ensemble. This variation is observed in both acceleration and displacement response spectra. Observing the ground motion set in its entirety, Figure 4(a) and (b) show the ratio of (m+σ)/m for acceleration and displacement spectra respectively, considering all ground motions. It may be observed from these plots that there is large dispersion of data among all ground motions when they characterized in terms of acceleration and displacement response spectra. The minimum ratio of (m+σ) to m for both acceleration and displacement spectra is more than 1.5. It is also interesting to note that this ratio remains almost constant, for both acceleration and displacement spectra, up to a period of approximately 2 seconds. Subsequently, the variation in displacement spectra is higher than acceleration spectra. Therefore, for structures with higher periods, larger dispersion in displacement response may be anticipated.

Table 2. Earthquake motions used for input in this study (Sommerville 2002).

(a) 50% in 50 Year Hazard Level

Earthquake& Date	**Mw**	**Station[1]**	**Distance (km)**	**Scale Factor**	**PGA[2] (g)**	**PGV[2] (cm/s)**	**PGD[2] (cm)**
Coyote Lake, 1979/6/8	5.7	Coyote Lake Dam (T)	4.0	1.395	0.39	29.8	3.6
		Gilroy # 6 (T)	1.2	0.999	0.47	49.6	7.1
Parkfield, 1966/6/27	6.0	Temblor (T)	4.4	1.143	0.64	44.3	5.0
		Array # 5 (T)	3.7	0.978	0.36	47.0	9.3
		Array # 8 (T)	8.0	2.302	0.56	25.6	8.2
Livermore, 1980/1/27	5.5	Fagundes Ranch (T)	4.1	1.644	0.39	23.9	5.1
		Morgan Territory Park (T)	8.1	2.958	0.39	23.8	5.6
Morgan Hill, 1984/4/24	6.2	Coyote Lake Dam (T)	0.1	0.673	0.75	40.5	3.2
		Anderson Dam Down (T)	4.5	0.572	0.26	14.0	3.5
		Halls Valley (T)	2.5	1.362	0.39	20.2	1.2

(b) 10% in 50 Year Hazard Level

Earthquake & Date	**Mw**	**Station[1]**	**Distance (km)**	**Scale Factor**	**PGA[2] (g)**	**PGV[2] (cm/s)**	**PGD[2] (cm)**
Loma Prieta, 1989/10/17	7.0	Los Gatos Pres Center (T)	3.5	1.016	0.74	92.5	16.6
		Saratoga Aloha Ave (T)	8.3	2.653	0.65	94.1	30.3
		Corralitos (T)	3.4	1.394	0.53	64.1	19.4
		Gavilan College (T)	9.5	2.097	0.66	63.2	12.9
		Gilroy historic		2.319	0.67	88.0	24.1
		Lexington Dam (T)	6.3	1.925	0.87	209.0	42.6
Kobe, Japan, 1995/1/17	6.9	Kobe JMA (T)	0.5	0.912	1.48	154.5	41.6
		Kobe JMA (L)	0.5	0.912	0.44	50.4	11
Tottori, Japan, 2000/10/6	6.6	Kofu (T)	10.0	1.039	0.78	94.6	22.1
		Hino (T)	1.0	0.827	0.85	145.9	83.7
Erzincan, Turkey, 1992/3/13	6.7	Erzincan (T)	1.8	2.455	0.69	32.6	6.2

(c) 2% in 50 Year Hazard Level

Earthquake & Date	Mw	Station[1]	Distance (km)	Scale Factor	PGA[2] (g)	PGV[2] (cm/s)	PGD[2] (cm)
Loma Prieta, 1989/10/17	7.0	Los Gatos Pres Center (T)	3.5	1.713	1.25	155.9	28.0
		Saratoga Aloha Ave (T)	8.3	4.473	1.09	158.6	51.1
		Corralitos (T)	3.4	2.350	0.89	108.0	32.7
		Gavilan College (T)	9.5	3.535	1.12	106.5	21.8
		Gilroy historic		3.910	1.14	148.4	40.6
		Lexington Dam (T)	6.3	3.245	1.48	352.4	71.9
		Lexington Dam (L)	6.3	3.245	1.41	83.0	12.3
Kobe, Japan, 1995/1/17	6.9	Kobe JMA (T)	0.5	1.537	2.50	260.5	70.1
Tottori, Japan, 2000/10/6	6.6	Kofu (T)	10.0	1.751	1.31	159.4	37.3
		Hino (T)	1.0	1.395	1.44	246.0	141.2
Erzincan, Turkey, 1992/3/13	6.7	Erzincan (T)	1.8	4.139	1.16	55.0	10.4

[1] T=Transverse, L=Longitudinal

[2] PGA = peak ground acceleration, PGV = peak ground velocity, PGD = peak ground displacement

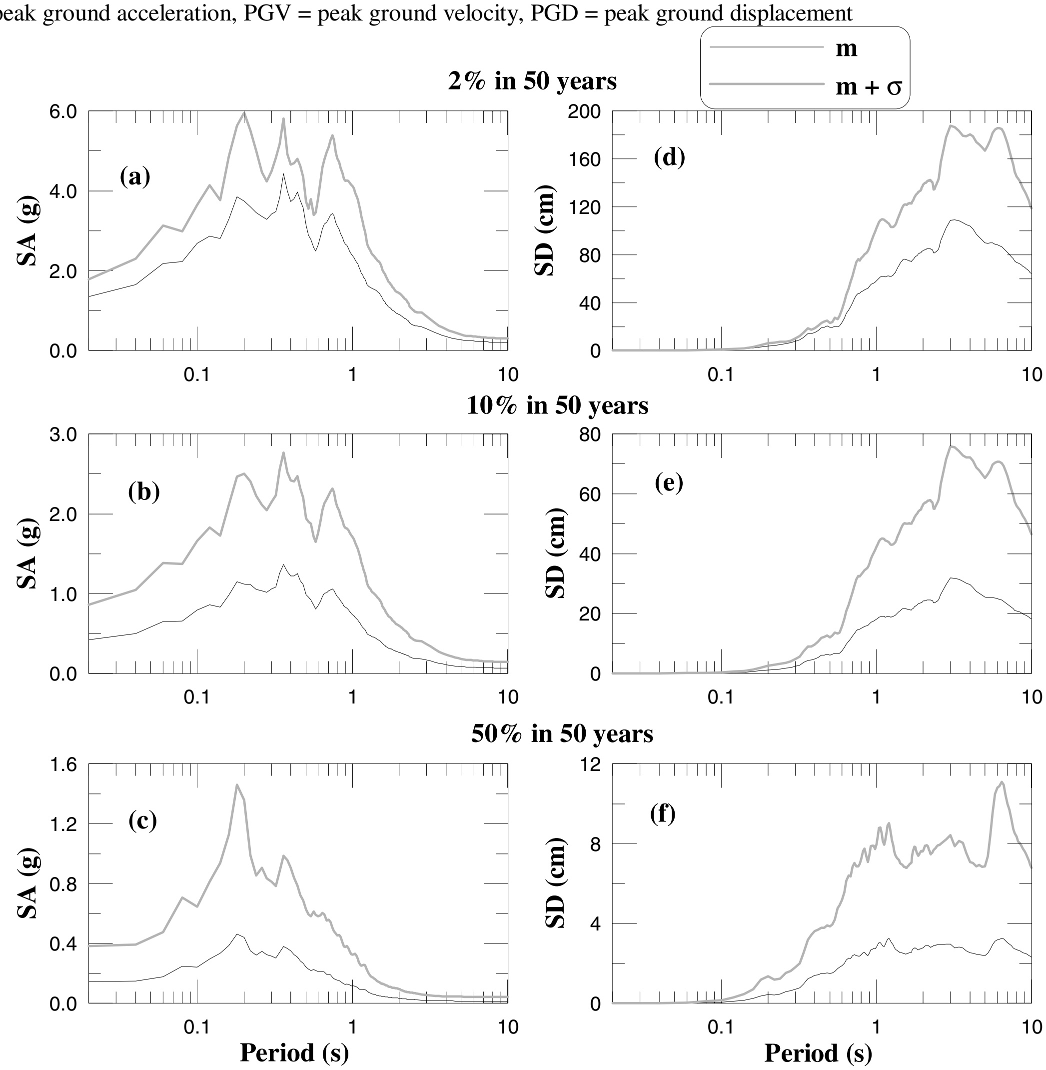

Figure 3. Summary 2% damped acceleration and displacement response spectrum, at different hazard levels, and in terms of mean m and mean plus one standard deviation (m+σ).

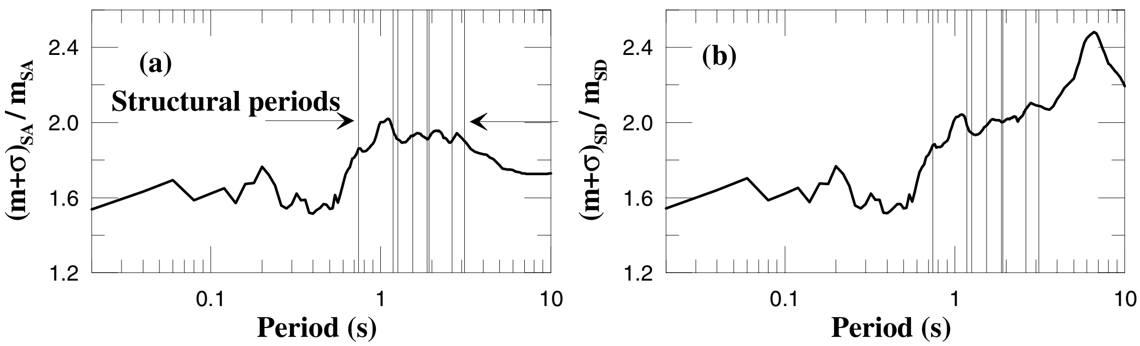

Figure 4. Normalized spectral characteristics (m+σ)/m: (a) acceleration spectrum and (b) displacement spectrum, considering all motions.

Nonlinear Dynamic Analyses Results

Nonlinear dynamic analyses are performed for all numerical models using OpenSees and considering the 32 ground motions previously described. Results from these analyses are summarized in Figure 5(a)-(h) in terms of the calculated peak horizontal floor acceleration (absolute) amplification (i.e. Ω = PHFA/PGA) versus normalized height. The normalized height h^* is taken as the floor height divided by the total height of building from the ground surface. These plots show the actual data of Ω obtained from the nonlinear analysis (NL analysis), their mean value m at each floor level, and the (m±σ) values, where σ is the standard deviation of each floor value. Also incorporated within these plots are the UBC 1997 and NEHRP 2000 code provisions for acceleration amplification distribution. These figures illustrate that the data does not follow any significant trend and more importantly, the code provisions do not provide a good estimate of Ω. In some cases the code recommendations are over conservative, while in other cases it under estimates the response. For example, the code specified values over estimate the floor level Ω for the upper floors in flexible buildings (i.e. the upper 50% of their height), while the code estimates are unconservative for the lower stories of rigid buildings (approximately from the base to 40% of their height).

To observe the extent of nonlinear behavior from these analyses, the displacement ductility demand μ_Δ (=Δ_{max} at the roof from the dynamic analysis divided by Δ_y from the pushover analysis) of the all the frames, is provided in Figure 6, as a function of the natural period. The m and (m+σ) values of μ_Δ are also plotted in these figures. With the exception of a few data points (excluded from the figure) μ_Δ is less than 6. It is also observed that as the period increases, μ_Δ reduces for both the flexible and rigid frames. For the 16 story buildings (both rigid and flexible), the mean ductility demand is approximately 1.0, illustrating that these models remained elastic or nearly elastic for all 32-ground motions. It may also be observed that the m and (m+σ) ductility demands for the flexible frames is higher than that of the rigid frames with the same number of stories. For the 4 story flexible building, the mean ductility demand is about 2.4, implying that this structure went to nonlinear zone for most of the motions. It is also interesting to note that there is a large dispersion in μ_Δ for both the flexible and rigid frames. The ratio of the m and (m+σ) ductility demand remains almost the same with increasing period, for both the flexible and rigid buildings.

Figure 5(a)-(h), illustrate that there is a large dispersion in the distribution of Ω, making it difficult to predict deterministically. Therefore, in this work, the framework of probability theory is applied, with the objective of associating a confidence level of an assumed acceleration amplification distribution with the analyses results. To do this it is assumed that the distribution of Ω, at a particular floor level is lognormal. Kolmogorov-Smirnov (KS) tests are carried out for each data set corresponding to the floor levels of all buildings and the probability (p-values), indicating the suitability of the lognormal hypothesis. The p-value is the probability of observing the given sample result under the assumption that the null hypothesis is true. If the p-value is less than the significance level α, then a previously assumed null hypothesis (lognormal distribution) has to be rejected. A significance level of α = 5% indicates the assumed lognormal distribution is reasonable. The lowest p-value obtained for any floor from these calculations was 0.20 (20%).

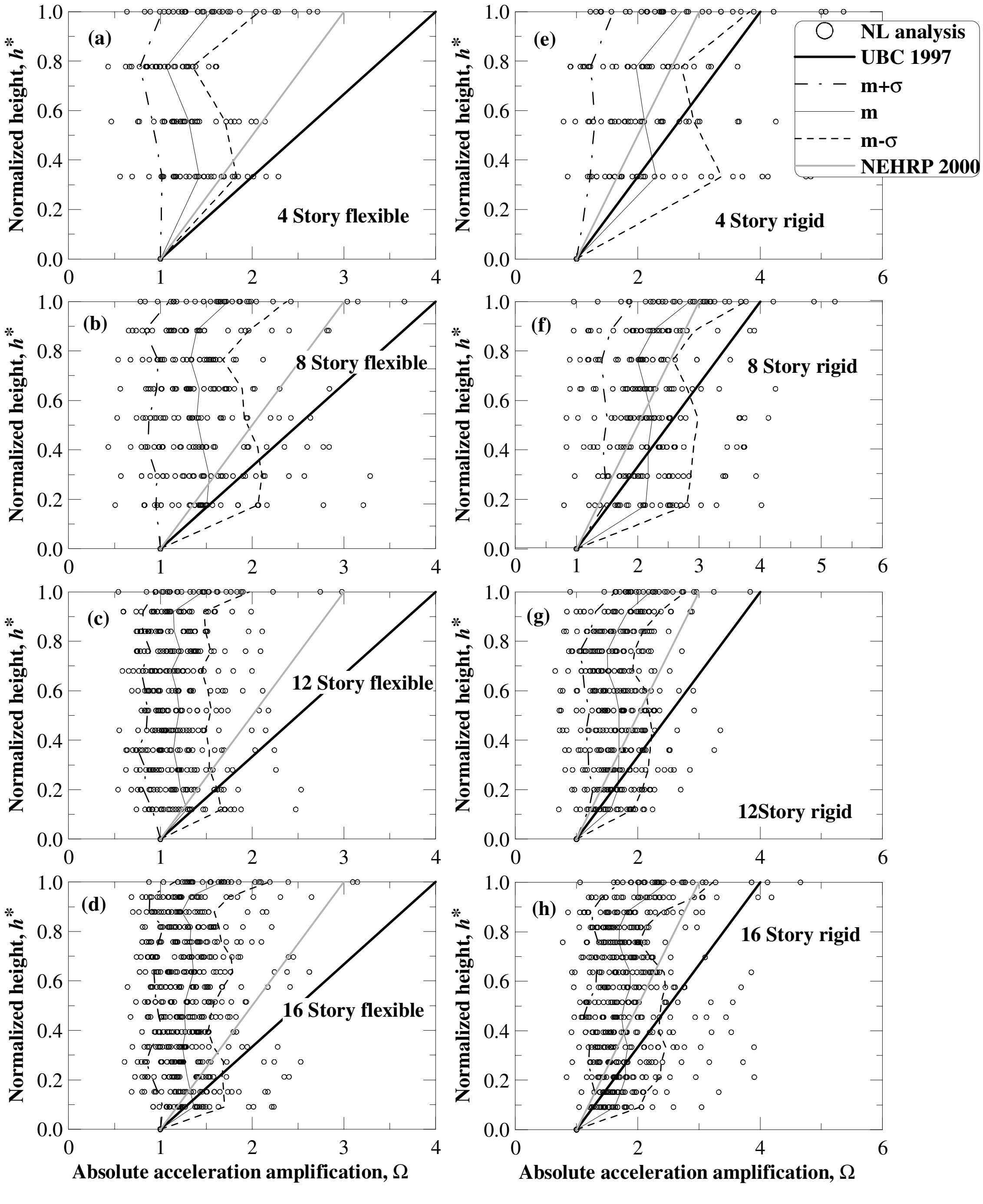

Figure 5. Distribution of absolute acceleration amplification for 4, 8, 12 and 16 story flexible and rigid frames.

Given the positive results from the KS tests, Ω is assumed to be log normally distributed and using the sample median and log standard deviation, the probability of not exceeding the code specified acceleration amplification distribution is calculated. Results from these confidence calculations are shown in Figure 7(a) and (b). It may be observed from Figure 7, that the code specified distribution under estimates the acceleration amplification at all lower floor levels. The normalized height at which the code begins to provide a conservative estimate of Ω differs significantly depending upon the desired confidence level (i.e. 50 or 90%). Moreover, it is interesting to note that the confidence level achieved is sensitive to the building type (flexible versus rigid) and the number of stories. Such factors are not accounted for in current code-based linear distributions.

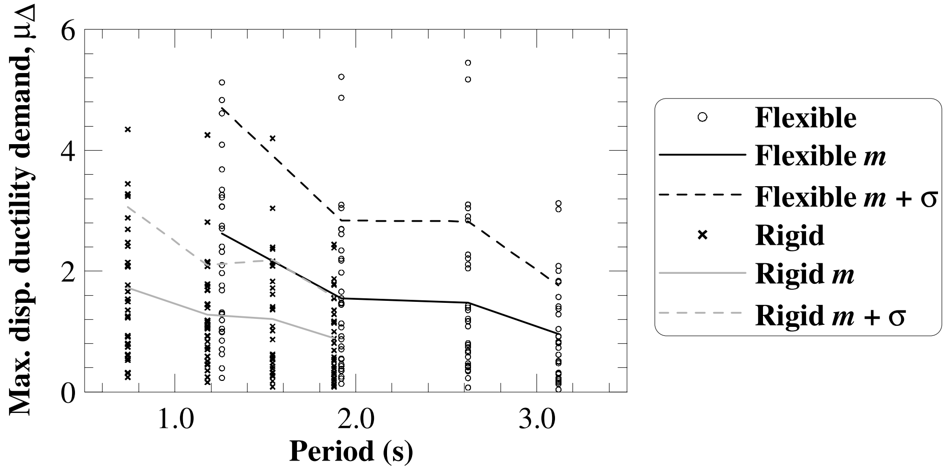

Figure 6. Ductility demand for flexible and rigid frames with 4, 8, 12 and 16 stories.

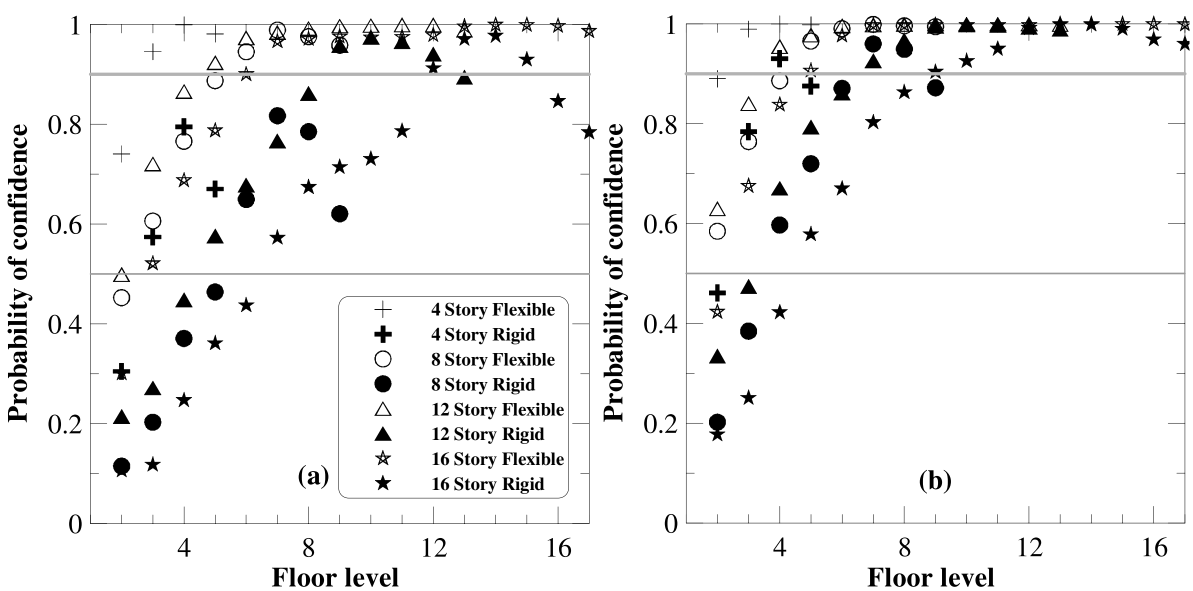

Figure 7. Probability of confidence considering: (a) NEHRP 2000 and (b) UBC 1997 recommendations.

Proposed Distribution

Figure 6(a)-(h) illustrates that the m and (m±σ) distribution of absolute acceleration amplification along the height for these buildings follows the same general "S" shaped curve. This implies that for all frames, shear-dominated behavior is observed at the bottom floors, flexural-dominated behavior is observed at the upper floors, and a combination of these two behaviors contributes to the middle floors level response. For these buildings, their fundamental mode shape resembles a shear-type behavior. Therefore, it is reasonable to assume that the shear behavior at the lower stories is attributed to first mode contributions, while the bending behavior in the upper stories is attributed to higher mode contributions. Since the scatter from the nonlinear analyses results is large, a simplified distribution for calculating the acceleration amplification Ω is desirable. In the strictest sense, an improved solution may consider the weighted contributions from the different modes. However, the resulting complicated analytical form may not be justified in light of the uncertainty associated with the ground motion (input), the building characteristics and other modeling assumptions. Therefore, in this paper, the following simplified expression is proposed:

$$\Omega = (1.0 + \alpha_1 \sqrt{h^*})(1.0 - h^*) + (\alpha_2 h^{*2}) h^* \tag{1}$$

where the coefficients α_1 and α_2 are empirical constants, which may be derived from the dynamic analyses results. Equation (1) is justified by considering the observed behavior from these analyses results as follows. The first term $(1.0 + \alpha_1 \sqrt{h^*})$, represents a parabolic distribution to emulate shear-dominated behavior at the lower floors, where Ω varies from 1.0 at the ground surface, i.e., h^* = 0 to Ω = $(1.0 + \alpha_1)$ at the roof, i.e., h^* = 1.0. The term $\alpha_2 h^{*2}$ emulates the bending-dominated behavior at the upper floors with Ω = α_2 at the roof, i.e., h^* = 1.0. To represent the decreasing shear contribution and simultaneously increasing bending contribution, with increased normalized height h^*, the terms $(1 - h^*)$ and h^* are multiplied by each of the terms in Equation (1). The proposed acceleration distribution profile captures the observations from these analyses very well, as illustrated in Figure 8. Figure 8(a) shows the individual analyses results, their mean values, and a best fit regression using Equation (1) to calculate Ω for the 8 story flexible building. These results are very encouraging, however, from a design perspective, it may be simpler to consider either all flexible or all rigid frames, providing an average sense of the distribution. Figure 8(b) considers this approach, whereby the average of all four flexible frame (mean) results are best fit the proposed distribution. In addition, the envelope (maximum) curve is provided, if a conservative estimate of Ω is more desirable. Although the distributions are promising, in simply comparing with mean analyses results (Figure 8), designers using such curves will not have a confidence level associated with their prediction. In other words, these curves do not guarantee, with some desired probability of confidence, that they will not exceed the nonlinear dynamic analysis solution (when an average or envelope is considered).

The framework of probability theory is again applied, whereby an assumed distribution is considered to allow the estimation of a confidence level for the desired prediction of the distribution of Ω. Assuming a lognormal distribution, two sets of curves are generated for this purpose (Figure 9). One set of curves ensures that using the proposed distribution (calculated with Equation (1) – solid lines), the Ω estimation will not be less than the *average* Ω from any floor considering these four buildings, with a given confidence level (50 or 90%). The other set of curves ensures that using the proposed distribution (calculated with Equation (1) – dashed lines), the Ω estimation will not be less than the *maximum* Ω from any floor considering these four buildings, again with a given confidence level (50 or 90%). Figure 9(a) and (b) shows these curves separated into either flexible or rigid building types, and compared with the code recommended distributions. Code recommended distributions are observed to be highly unconservative in some cases when a 50% or 90% confidence level is desired. The coefficients α_1 and α_2 for the average and envelope curves obtained from actual nonlinear analysis data and also for the proposed curves (assuming a lognormal distribution) are given in Table 3. It is important to point out that these values are based on the selected eight building frames and the ground motions considered in this study.

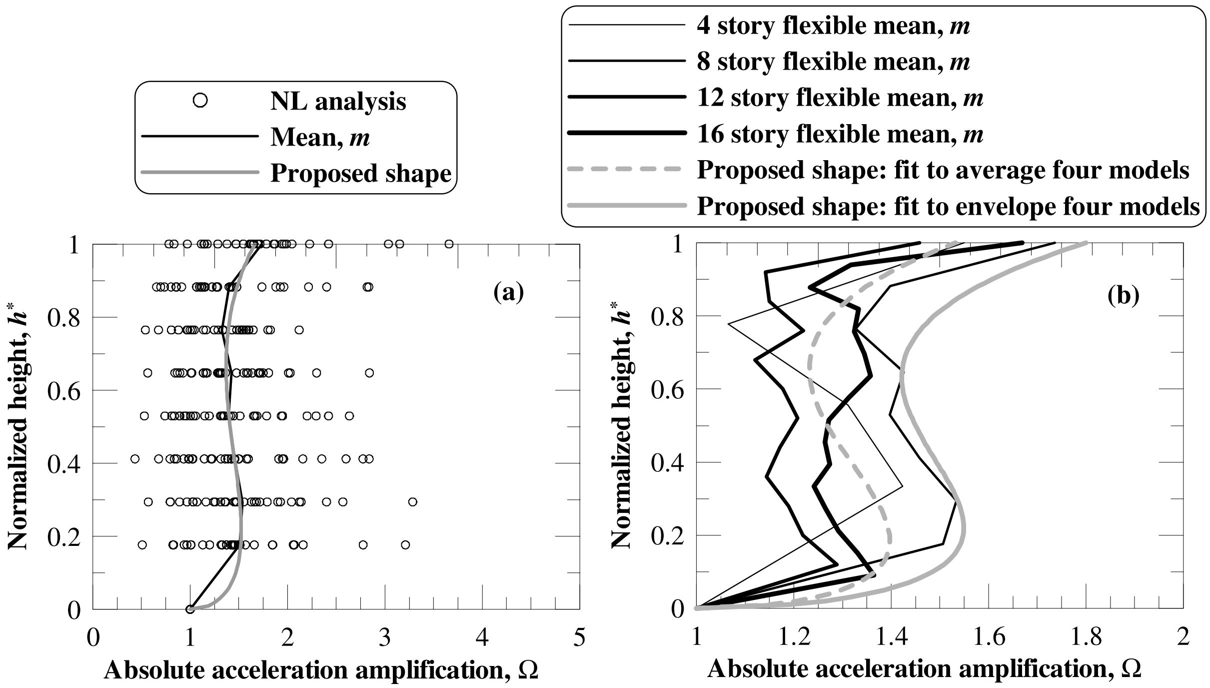

Figure 8. Sample results from proposed distribution: (a) compared with individual analyses and mean of these analyses for the 8 story flexible building and (b) compared with the mean of the analyses, for all flexible frames (an average and envelope curve is illustrated).

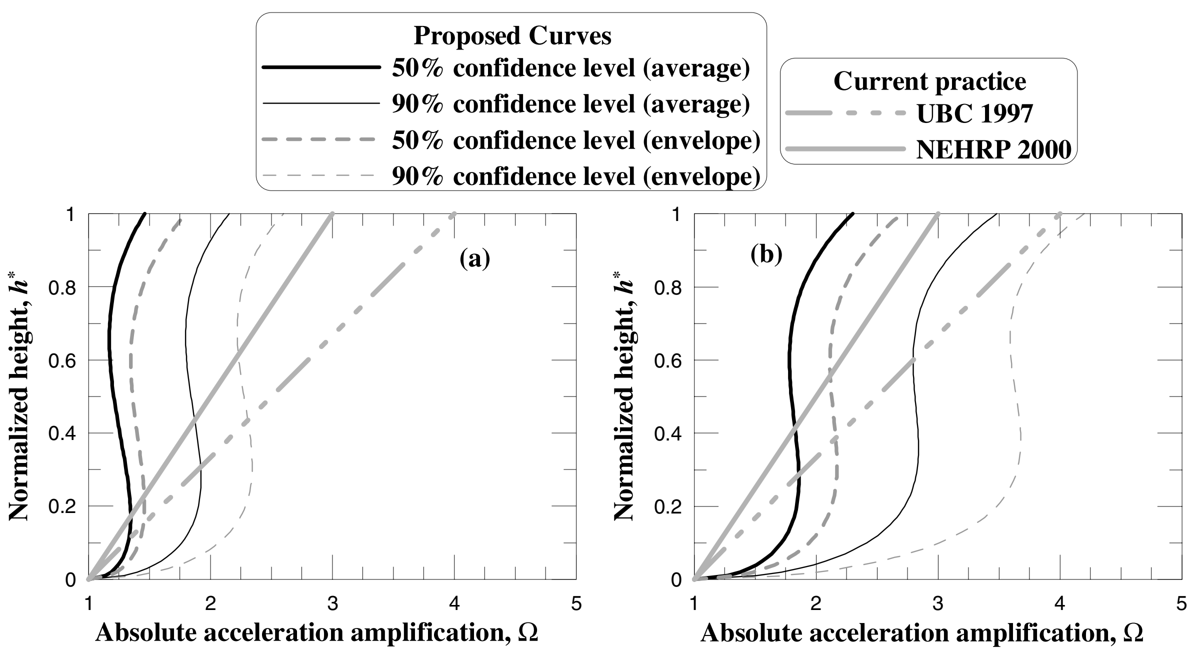

Figure 9. Proposed acceleration amplification distribution along the normalized height for: (a) flexible and (b) rigid buildings.

Table 3. Regression coefficients α_1 and α_2 as obtained from these analysis.

Flexible Buildings						
	Dynamic Analyses Results		Proposed (Equation 1)			
			50% probability of confidence[1]		90% probability of confidence	
	Average	Envelope	Average	Envelope	Average	Envelope
α_1	1.63	2.05	1.48	3.03	1.80	4.10
α_2	1.53	1.80	1.46	2.16	1.80	2.60
Rigid Buildings						
	Dynamic Analyses Results		Proposed (Equation 1)			
			50% probability of confidence		90% probability of confidence	
	Average	Envelope	Average	Envelope	Average	Envelope
α_1	3.12	3.95	2.85	5.31	3.65	7.40
α_2	2.42	2.85	2.30	3.48	2.70	4.20

[1] Probability of confidence estimates are calculated assuming a lognormal Ω distribution

SUMMARY REMARKS AND CONCLUSIONS

In this study, the distribution of the peak horizontal floor acceleration (PHFA) along the height of building structures is investigated using a large number of ground motions, with a broad range of seismic hazard levels. Eight representative steel moment-resisting frame buildings are considered, representing actual buildings found on the West coast of the U.S. The structures consider represent a broad range of fundamental periods (T_1 = 0.71 – 3.09 seconds) and both flexible and rigid building types. An ensemble of 32 different earthquake time histories is used as input to numerical models of these buildings, with nonlinearity incorporated at beam-column joints, as commonly anticipated in design practice. Although there is significant scatter in the resulting acceleration amplification distribution, a lognormal distribution on a per floor basis is shown to reasonably estimate the ensemble floor distributions. Using the lognormal assumption, confidence levels are calculated based on UBC and NEHRP code recommendations. Finally, a proposed acceleration amplification distribution, with an associated confidence level, is presented such that the probability of exceeding a limit state of Ω is reduced considering all floors. Since seismic fragility curves used in design are often provided in terms of PHFA, the proposed curves can be directly used to estimate the vulnerability of acceleration-sensitive nonstructural components. Furthermore, the proposed distribution can also be used to estimate the force for attached nonstructural components housed within similar types of buildings and considering the range of ground motions from this study.

ACKNOWLEDGEMENTS

Support of this work was provided in part by the Earthquake Engineering Research Centers Program of the National Science Foundation, under Award Number EEC-9701568 through the Pacific Earthquake Engineering Research Center (PEER). The above support is greatly appreciated.

REFERENCES

1. Adam, C, Fotiu, PA. "Dynamic response of earthquake excited inelastic primary-secondary systems, Paper No. 0310, *Proc. 12th World Conf. Earthq. Eng.,* Auckland, New Zealand, New Zealand Society of Earthquake Engineering, Upper Hutt, New Zealand. 2000.

2. Ayers, JM, Sun TY, Brown, FR. "Nonstructural damages to buildings," *The Great Alaska Earthquake of 1964: Engineering*, National Academy of Science, Washington, D.C. 1973.
3. Ayers, JM, Sun TY. "Nonstructural damages," San Fernando, California, earthquake of February 9, 1971," *U.S. Dept. of Commerce*, National Oceanic and Atmospheric Admin., Vol. 1. 1973.
4. Aziz, T, Ghobarah, A. "Equipment design: Future directions," *Proc. 9th World Conf. Earthq. Eng*., Tokyo-Kyoto, Japan, Aug. 2-9, Japan Assoc. for Earthq. Disaster Prevention, Tokyo, 6, 261-266. 1988.
5. Igusa, T. "Response characteristics of inelastic 2-DOF primary-secondary systems," *J. Eng. Mech., ASCE*, 116 (5), 1160-1174. 1990.
6. Kehoe, BE, Freeman, SA. "A critique of procedures for calculating seismic design forces for nonstructural elements," *Proc. Seminar on Seismic Design, Retrofit, and Performance of Equipment and Nonstructural Components* (ATC-29-1), Applied Technology Council, pp. 57-70. 1998.
7. Lin, J, Mahin, SA. "Seismic response of light subsystems on inelastic structures," *J. Struc. Eng. ASCE*, 111 (2), 400-417. 1985.
8. Miranda, E, Taghavi, S. "Estimation of seismic demands on acceleration sensitive nonstructural components in critical facilities**"** *Proc. Seminar on Seismic Design, Retrofit, and Performance of Nonstructural Components, ATC-29-2*, Applied Technology Council, Newport beach, California, pp-347-360. 2003.
9. *NEHRP Recommended Provisions for Seismic Regulations for New Buildings*. 2000 Edition, Building Seismic Safety Council, Washington, D.C., May. 2000.
10. OpenSees. *Open System for Earthquake Engineering Simulation*. Pacific Earthquake Engineering Research (PEER) Center. University of California, Berkeley. On-line documentation at: http://opensees.berkeley.edu/. 2003.
11. Phipps, MT. "The impact of nonstructural damage on building performance: reflections on the 1994 Northridge earthquake." *Report UCB/EERC- 97/05*, The EERC-CUREe Symposium in Honor of Vitelmo V. Bertero, Earthquake Engineering Research Center, University of California, Berkeley, California, 173-178. 1997.
12. Reitherman, R, Sabol, TA. "Northridge earthquake of January 17, 1994: reconnaissance report - nonstructural damage." *Earthquake Spectra*, EERI, 11 (Supp), 453-514. 1995.
13. Rihal, SS. "Performance and behavior of non-structural building components during the Whittier Narrows, California (1987) and Loma Prieta, California (1989) earthquakes: selected case studies," *Report No. ATC-29*, *Proc. Seminar and Workshop on Seismic Design and Performance of Equipment and Nonstructural Elements in Buildings and Industrial Structures*, Applied Technology Council, Redwood City, California, pp. 119-143. 1992.
14. Santa-Ana, PR, Miranda, E. "Strength Reduction Factors for Multi-degree-of-freedom systems." In *12th world conference on earthquake engineering (WCEE 2000).* 2000.
15. Schroeder, ME, Backman, RE. "Analytical studies in support of the 1994 NEHRP provisions for nonstructural components." *5th U.S. Nat. Conf. Earthq. Eng*., July 10-14, Chicago, Ill., Earthquake Engineering Research Institute, Oakland, Calif., 4, 755-764. 1994.
16. Searer, GR, Freeman, SA. "Unintended consequences of code modification," *Proc. 7th U.S. National Conference on Earthquake Engineering*, EERI, Boston, Massachusetts, CD-Rom. 2002.
17. Sewell, RT, Cornell, CA, Toro, GR, McGuire, RK, Kassawara, RP, Singh, A, Stepp, JC. "Factors influencing equipment response in linear and nonlinear structures," *Trans. 9th Int. Conf. Struc. Mech. Reactor Tech*., Aug. 17-21, Lausanne, Switzerland, A. A. Balkema, Rotterdam, K2, 849-856. 1989.
18. Singh, MP, Suarez, LE, Matheu, EE, Maldonado, GO. "Simplified procedure for seismic design of nonstructural components and assessment of current code provisions." Report NCEER-93-0003, National Center for Earthquake Engineering Research, State University of New York at Buffalo, March 1. 1993.

19. Sommerville, P. "Ground motion time histories for the UC lab building." Unpublished PEER (Pacific Earthquake Engineering Research) Center Report. 2002.
20. Soong, TT. "Seismic performance of nonstructural elements during the Loma Prieta earthquake." Report NIST SP 796, Proc., 22nd Joint Meeting U.S.-Japan Cooperative Program in Natural Resources Panel on Wind and Seismic Effects, Natl. Inst. of Standards and Technology, Gaithersburg, Maryland, 331-336. 1990.
21. Soong, TT, Shen, G, Wu, Z, Zhang, RH, Grigoriu, M. "Assessment of the 1991 NEHRP provisions for nonstructural components and recommended revisions." *Report NCEER-93-0003*, National Center for Earthquake Engineering Research, Buffalo, N.Y. 1993.
22. Toro, GR, McGuire, RK, Cornell, CA, Sewell, RT. Linear and nonlinear response of structures and equipment to California and Eastern United States earthquakes, Report NP-5566, Electric Power Research Institute, Palo Alto, Calif., Aug. 1989.
23. *Uniform Building Code*. Vol. 2: Structural Engineering Design provisions, International Conference of Building Officials, Whittier, Calif., May 1994.
24. *Uniform Building Code*. Vol. 2: Structural Engineering Design provisions, International Conference of Building Officials, Whittier, Calif., Aug. 1997.
25. Whitman, RV, Hong, ST, Reed, J. "Damage statistics for high-rise buildings in the vicinity of the San Fernando Earthquake," Report No. 7, Massachusetts Institute of Technology, 204 pages. 1973.